Original Article | Genitourinary Imaging

eISSN 2005-8330
https://doi.org/10.3348/kjr.2020.0865
Korean J Radiol 2021;22(5):735-741

Korean Journal of Radiology
KJR

Circularity Index on Contrast-Enhanced Computed Tomography Helps Distinguish Fat-Poor Angiomyolipoma from Renal Cell Carcinoma: Retrospective Analyses of Histologically Proven 257 Small Renal Tumors Less Than 4 cm

Hye Seon Kang[1], Jung Jae Park[1, 2]

[1]Department of Radiology, Chungnam National University Hospital, Daejeon, Korea; [2]Department of Radiology, Chungnam National University College of Medicine, Daejeon, Korea

Objective: To evaluate circularity as a quantitative shape factor of small renal tumor on computed tomography (CT) in differentiating fat-poor angiomyolipoma (AML) from renal cell carcinoma (RCC).

Materials and Methods: In 257 consecutive patients, 257 pathologically confirmed renal tumors (either AML or RCC less than 4 cm), which did not include visible fat on unenhanced CT, were retrospectively evaluated. A radiologist drew the tumor margin to measure the perimeter and area in all the contrast-enhanced axial CT images. In each image, a quantitative shape factor, circularity, was calculated using the following equation: $4 \times \pi \times (\text{area} \div \text{perimeter}^2)$. The median circularity (circularity index) was adopted as a representative value in each tumor. The circularity index was compared between fat-poor AML and RCC, and the receiver operating characteristic (ROC) curve analysis was performed. Univariable and multivariable binary logistic regression analysis was performed to determine the independent predictor of fat-poor AML.

Results: Of the 257 tumors, 26 were AMLs and 231 were RCCs (184 clear cell RCCs, 25 papillary RCCs, and 22 chromophobe RCCs). The mean circularity index of AML was significantly lower than that of RCC (0.86 ± 0.04 vs. 0.93 ± 0.02, $p < 0.001$). The mean circularity index was not different between the subtypes of RCCs (0.93 ± 0.02, 0.92 ± 0.02, and 0.92 ± 0.02 for clear cell, papillary, and chromophobe RCCs, respectively, $p = 0.210$). The area under the ROC curve of circularity index was 0.924 for differentiating fat-poor AML from RCC. The sensitivity and specificity were 88.5% and 90.9%, respectively (cut-off, 0.90). Lower circularity index (≤ 0.9) was an independent predictor (odds ratio, 41.0; $p < 0.001$) for predicting fat-poor AML on multivariable logistic regression analysis.

Conclusion: Circularity is a useful quantitative shape factor of small renal tumor for differentiating fat-poor AML from RCC.

Keywords: *Angiomyolipoma; Renal cell carcinoma; Computed tomography; Differential diagnosis; Circularity*

INTRODUCTION

Angiomyolipoma (AML) is the most common benign renal tumor, which is pathologically composed of fat, muscle, and vessels [1,2]. A typical AML is easily diagnosed because of its abundant fat, which is detectable on unenhanced computed tomography (CT) images [3,4]. However, approximately 4.5% of AMLs are difficult to diagnose due to the lack of identifiable fat on CT images [5,6]. Therefore, fat-poor AML may be diagnosed only after a biopsy or

Received: July 2, 2020 **Revised:** September 5, 2020 **Accepted:** October 8, 2020
Corresponding author: Jung Jae Park, MD, Department of Radiology, Chungnam National University Hospital, Chungnam National University College of Medicine, 282 Munhwa-ro, Jung-gu, Daejeon 35015, Korea.
• E-mail: jjskku@naver.com

surgery because this lesion can be misdiagnosed as renal cell carcinoma (RCC) on CT or even on magnetic resonance imaging [7].

In comparison with RCC, fat-poor AML occurs more frequently in women [8]. On CT imaging, fat-poor AML shows higher attenuation on unenhanced images and more homogeneous and prolonged enhancement after contrast enhancement compared with RCC [9-11]. Moreover, tumor shape is another important diagnostic point to differentiate fat-poor AML from RCC across imaging techniques. Round shapes may suggest increased possibility of malignancy [12]. On the contrary, fat-poor AML may be accompanied by lobulations or indentations along the tumor margin, which diminish the roundness due to the soft tissue composition. In association with tumor morphology, several studies have reported distinctive radiologic patterns to diagnose fat-poor AML, such as angular interface, ice-cream cone sign, or overflowing beer sign [13-15]. However, majority of these studies evaluated the tumor shape in a qualitative or semi-quantitative manner, which might decrease reliability and reproducibility. Furthermore, the radiologic signs for AML revealed relatively low sensitivity for predicting tumor benignity because the signs might not be apparent in several AMLs despite the non-round features [15]. Therefore, the quantitative morphologic assessment for tumor roundness may warrant a reliable decision for small renal tumors with improved diagnostic accuracy.

Circularity is a quantitative measure of how closely an object resembles a perfect circle on a two-dimensional plane. It is calculated by using the perimeter and area of a figure on a plane according to the following equation: $4 \times \pi \times (\text{area} \div \text{perimeter}^2)$. The maximum value of circularity is one in a perfect circle and any feature that diminishes roundness, such as angulations, elongations, and eccentricity, may decrease the value [16]. Therefore, circularity might be a potential shape factor that can quantitatively evaluate the roundness of a tumor shape. Previously, several studies utilized circularity to evaluate nuclear morphology in microscopic findings, especially in RCCs [17-19]. However, to the best of our knowledge, no study has attempted to utilize circularity in a morphologic analysis on macroscopic imaging. We hypothesized that tumor circularity determined on cross-sectional CT images might be useful for differentiating AML from RCC in small renal tumors. Therefore, this study aimed to evaluate the usefulness of circularity as a quantitative shape factor of small renal tumors on CT in differentiating fat-poor AML from RCC.

MATERIALS AND METHODS

Patients

Our Institutional Review Board approved this retrospective study and the requirement for informed consent was waived (IRB No. 2020-06-094-001). Between January 2007 and December 2017, 623 patients underwent surgery or intra-operative radiofrequency ablation (RFA) with biopsy in our hospital, under the radiologic suspicion of RCC. Of these patients, we selected 575 patients who met the following inclusion criteria: a single sporadic renal tumor, pathologically confirmed RCC (clear cell, papillary, and chromophobe type) or AML on surgical or biopsy specimen, and available preoperative CT imaging composed with unenhanced and contrast-enhanced images acquired within 3 months before treatment. A genitourinary radiologist (8 years of experience in genitourinary CT imaging) initially evaluated preoperative CT images and 318 patients were excluded as per the following exclusion criteria: inadequate image quality due to insufficient scan range, thick slice thickness (> 5 mm), or artifact (n = 27), non-small size tumor (maximum diameter ≥ 4 cm on imaging) (n = 282), or visible fat component within the tumor on unenhanced images (n = 9). Finally, 257 renal tumors in 257 patients were included in this study (Fig. 1).

Data Collection

Clinical data, such as patients' sex and age at the time of treatment, were recorded. Pathologic data were

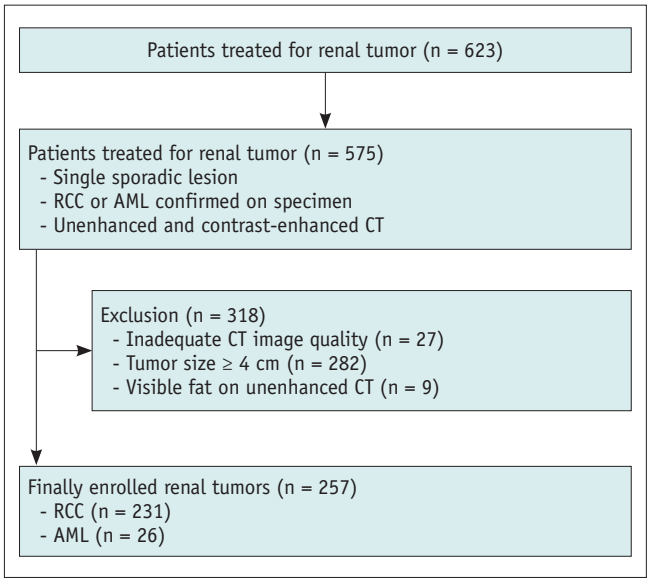

Fig. 1. Flowchart of the study enrollment. AML = angiomyolipoma, CT = computed tomography, RCC = renal cell carcinoma

https://doi.org/10.3348/kjr.2020.0865

Korean Journal of Radiology
KJR

retrospectively acquired by reviewing the pathologic reports, which were determined by a genitourinary pathologist. All included patients had preoperative CT imaging composed of unenhanced images and at least one phase of post-contrast images. Of the 257 enrolled patients, 162 (63%) received CT examination in our hospital and the remaining patients (37%) received CT examination in other hospitals. Because of the heterogeneity in the CT equipment and imaging protocols, we only considered the inclusion and exclusion criteria regarding imaging quality.

Image Analysis

All CT images were evaluated by a radiologist with 8 years of experience in genitourinary CT imaging. The clinical and pathologic data were blinded to minimize bias. Before the imaging analysis, the radiologist selected one phase of contrast-enhanced imaging in which the tumor margin was clearly demarcated from the adjacent normal tissue among the multi-phase contrast-enhanced images.

The set of selected contrast-enhanced axial images were transferred to the public domain image processing program ImageJ and were then analyzed [20]. The radiologist placed a region of interest along the tumor margin in all the axial images that encompassed the lesion. The area and perimeter of the tumor was recorded and the circularity was automatically calculated according to the following equation: $4 \times \pi \times (\text{area} \div \text{perimeter}^2)$. The median value of circularity (circularity index) was adopted as a representative value in a tumor instead of the mean value, because circularities measured in the superior and inferior pole of the tumor were substantially distorted due to partial volume effect. A second radiologist (with 3 years of experience in CT imaging) independently evaluated the images in a similar manner to determine inter-reader agreement in measuring tumor circularity.

The lesions were qualitatively analyzed regarding the presence of any imaging features in association with fat-poor AML, such as angular interface, ice-cream cone signs, or overflowing beer signs [13-15]. The radiologist used a four-point grading scale, defined as follows: score of 1, definitely absent; score of 2, probably absent; score of 3, probably present; score of 4, definitely present. The second radiologist also evaluated the images using the same method to determine inter-reader agreement.

Statistical Analysis

Statistical analysis was performed using the Predictive Analytics Software (SPSS version 20.0; IBM Corp.). Clinical and pathologic findings were compared between the patients with fat-poor AML and those with RCC using the independent *t* test, Mann-Whitney U test, or Fisher exact test. The circularity index was compared between fat-poor AML and RCC using the independent *t* test and it was compared between RCC subtypes using the one-way analysis of variance. Receiver operating characteristic (ROC) curve analysis was performed to determine the diagnostic performance of variables in differentiating fat-poor AML from RCC. The optimal cut-off value was determined by calculating the Youden index on the curve, and the diagnostic parameters such as sensitivity and specificity were calculated according to the cut-off value. The DeLong test was used to compare the area under the curve (AUC) between the circularity index and radiologic features for AML. Univariable and multivariable binary logistic regression analyses were performed to determine the independent predictor of fat-poor AML among the clinical and radiologic variables. The agreement of measurements between the two radiologists was determined using the intra-class correlation coefficient (ICC) for evaluating circularity and κ values for determining presence of any radiologic sign for AML. A two-sided p value < 0.05 indicated statistical significance.

RESULTS

Among the 257 patients, 102 (39.7%) and 88 (34.2%) patients received radical and partial nephrectomy, respectively. The remaining 67 (26.1%) patients received intra-operative RFA with biopsy. Of the 257 tumors, 26 (10.1%) were AMLs and 231 (89.9%) were RCCs (184 clear cell RCCs, 25 papillary RCCs, and 22 chromophobe RCCs). Table 1 describes the clinical characteristics of the enrolled patients. The mean age was not significantly different between the patients with fat-poor AML and those with RCC (p = 0.21). However, fat-poor AML was more prevalent

Table 1. Clinical Characteristics

	Fat-Poor AML	RCC	*P*
Mean age (years)	56.9 ± 10.2	59.6 ± 12.0	0.212
Sex			< 0.001
Male	7	163	
Female	19	68	
Mean tumor volume (cc)	3.3 ± 4.3	9.6 ± 8.0	< 0.001
Mean tumor diameter (cm)	1.7 ± 0.8	2.3 ± 0.9	< 0.001

Data are mean ± standard deviations or numbers. AML = angiomyolipoma, RCC = renal cell carcinoma

https://doi.org/10.3348/kjr.2020.0865

in women ($p < 0.001$), and the mean tumor volume was significantly smaller in AMLs than in RCCs ($p < 0.001$).

The circularity index was lower in AML (mean, 0.86; standard deviation [SD], 0.04) than in RCC (mean, 0.93; SD, 0.02). The difference was statistically significant ($p < 0.001$). The mean circularity index of clear cell, papillary, and chromophobe RCCs were 0.93 (SD, 0.02), 0.92 (SD, 0.02), and 0.92 (SD, 0.02), respectively. The circularity index was not statistically different between each pathologic type of RCCs (Fig. 2).

In the ROC curve analysis to differentiate fat-poor AML from RCC, the AUC of the circularity index was 0.924 (95% confidence interval [CI], 0.88–0.95) and the optimal cut-off was 0.90 ($p < 0.001$). With the cut-off, the sensitivity and specificity were 88.5% (69.8–97.6%) and 90.9% (95% CI, 86.4–94.3%), respectively. The AUC of any presenting sign for AML was 0.820 (95% CI, 0.77–0.87) and the sensitivity and specificity were 65.4% (95% CI, 44.3–82.8%) and 89.6% (95% CI, 85.4–93.6%), respectively (cut-off, ≥ 3 points; $p < 0.001$). The AUC of tumor volume was 0.801 (95% CI, 0.75–0.85) and the cut-off was 5.8 cc ($p < 0.001$).

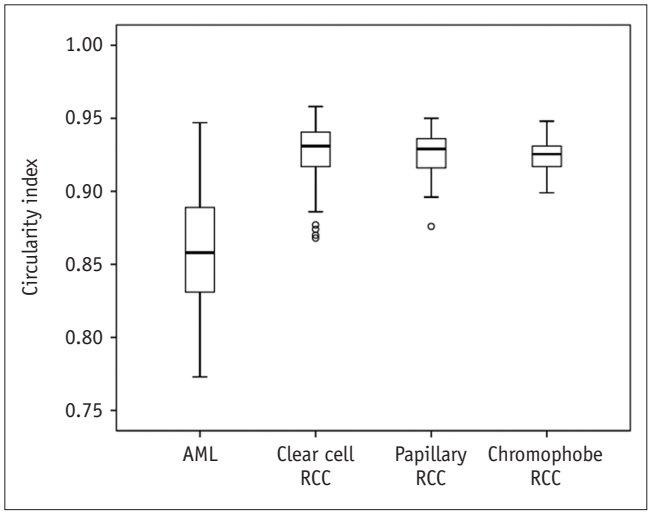

Fig. 2. Box-and-whisker plot shows the relationship between circularity index and tumor pathology. AML = angiomyolipoma, RCC = renal cell carcinoma

With the cut-off, the sensitivity and specificity were 88.5% (95% CI, 69.8–97.6%) and 59.7% (95% CI, 53.1–66.1%), respectively. The comparison of AUCs between circularity index and any presenting sign for AML, revealed a statistically significant difference ($p = 0.001$). Inter-reader agreement was excellent for evaluating tumor circularity on CT images (ICC, 0.84) and determining presence of radiologic sign for AML (κ, 0.87).

In the univariable and multivariable binary logistic regression analysis, female sex (odds ratio [OR], 6.46; $p = 0.003$), lower tumor volume (OR, 6.58; $p = 0.012$), and lower circularity index (OR, 41.0; $p < 0.001$) were independent predictors of fat-poor AML (Table 2).

Table 3 shows the results of qualitative analysis regarding the presence of any sign for AML, such as angular interface, ice-cream cone sign, or overflowing beer sign. Of the 26 AMLs, 17 AMLs (65.4%) revealed radiologic signs of AML and 207 of 231 RCCs (89.6%) did not reveal any sign of AML (Fig. 3). The AMLs with radiologic signs of AML revealed lower mean circularity index than those without (0.84 ± 0.03 vs. 0.89 ± 0.04; $p < 0.001$).

DISCUSSION

Our study demonstrated that tumor circularity on axial CT images could be useful for differentiating fat-poor AML from RCC in small renal tumors. Lower circularity measured on a cross-sectional CT image revealed a higher possibility of fat-poor AML, and circularity was found to be an independent predictor of AML in our study cohort.

Table 3. Results of Qualitative Analysis of Tumor Morphology

	Fat-Poor AML (n = 26)	RCC (n = 231)
Radiologic sign for AML*		
Present	17 (65.4)	24 (10.4)
Absent	9 (34.6)	207 (89.6)

Data in parentheses are percentages. *Presence of any pattern such as angular interface sign, ice-cream cone sign, or overflowing beer sign. AML = angiomyolipoma, RCC = renal cell carcinoma

Table 2. Results of Logistic Regression Analysis for Predicting Fat-Poor AML

	Univariable Analysis		Multivariable Analysis	
	OR	*P*	OR	*P*
Sex (female)	6.51 (2.62–16.21)	< 0.001	6.46 (1.86–22.40)	0.003
Tumor volume (≤ 5.8 cc)	11.42 (3.32–39.04)	< 0.001	6.58 (1.51–28.71)	0.012
Circularity index (≤ 0.9)	76.70 (21.2–277.04)	< 0.001	41.02 (6.58–255.25)	< 0.001
Radiologic sign for AML*	19.41 (7.63–49.40)	< 0.001	1.42 (0.27–7.48)	0.683

Data in parentheses are 95% confidence intervals. *Presence of any pattern such as angular interface sign, ice-cream cone sign, or overflowing beer sign. AML = angiomyolipoma, OR = odds ratio

https://doi.org/10.3348/kjr.2020.0865

Korean Journal of Radiology
KJR

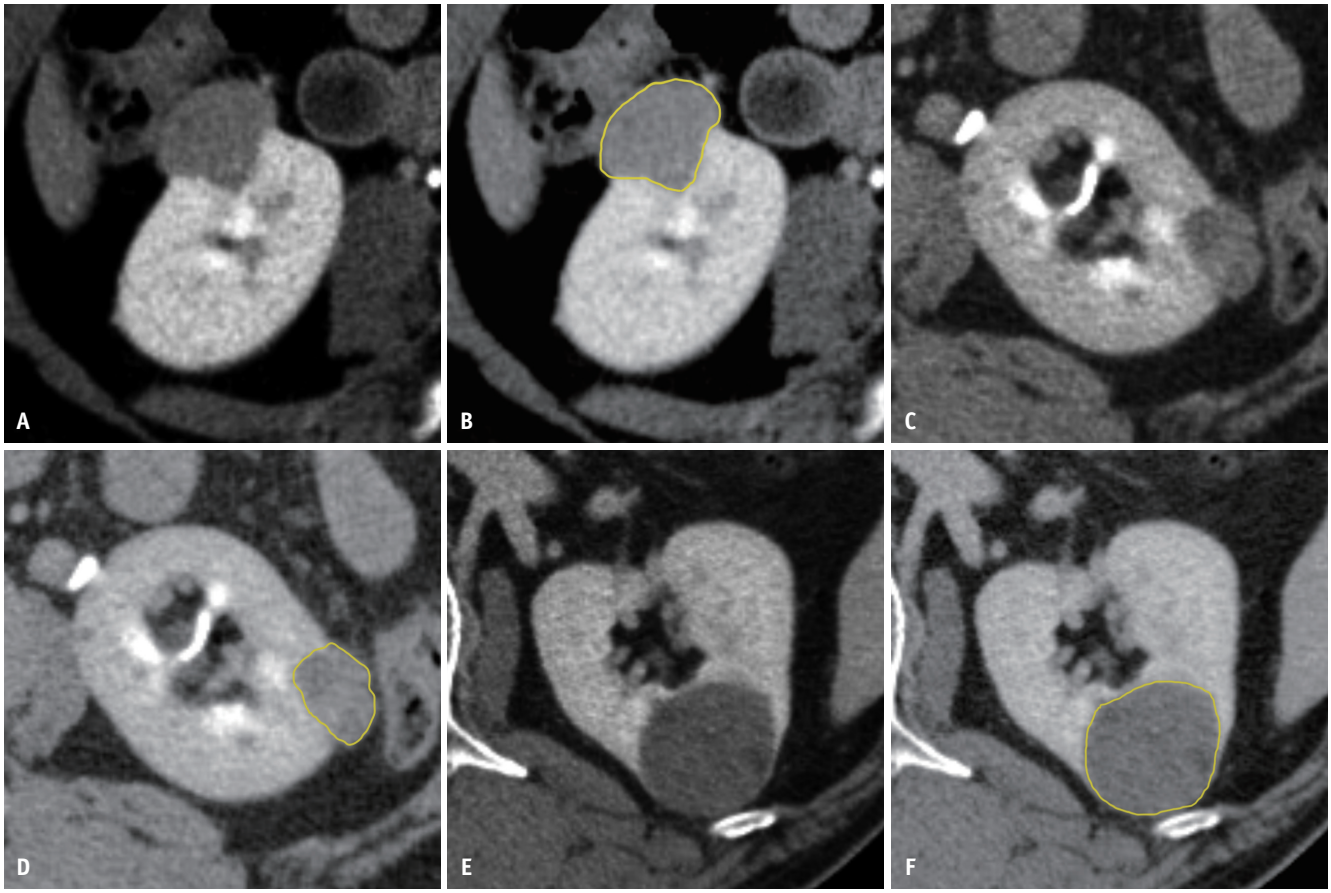

Fig. 3. Radiologic signs of AML.
A, B. A 52-year-old female with AML. The non-round shaped tumor shows an ice-cream cone sign with angular interface. The circularity on this plane was 0.82 (area, 70.94 mm^2; perimeter, 33.0 mm) and the circularity index was 0.85. **C, D.** A 45-year-old female with AML. The non-round shaped tumor does not show any distinct sign for AML. The circularity of the non-round shaped tumor on this plane was 0.84 (area, 119.58 mm^2; perimeter, 42.4 mm) and the circularity index was 0.83. **E, F.** A 60-year-old male with papillary renal cell carcinoma. The circularity of the round shaped tumor on this plane was 0.94 (area, 280.82 mm^2; perimeter, 61.3 mm) and the circularity index was 0.94. AML = angiomyolipoma

In studies that retrospectively analyzed pathologic outcomes of small renal tumors without visible fat on CT imaging, about 8 to 14% of the tumors were confirmed as AMLs after biopsy or surgery [14,15,21-23]. In line with previous results, 10.1% of small renal tumors were treated unnecessarily with surgery or RFA in our hospital, although they were actually benign AMLs. Therefore, fat-poor AML seems to be a diagnostic challenge and these findings may warrant further exploration of the imaging findings or techniques for better diagnosis.

Tumor shape on cross-sectional imaging is sometimes useful for differentiating fat-poor AML from RCC. Verma et al. [13] initially reported that the presence of an angular interface between a lesion and the renal parenchyma was indicative of benign renal tumor with high specificity and positive predictive value. Kim et al. [14] introduced the imaging feature of an exophytic renal tumor showing the angular interface as an "ice-cream cone" sign; they demonstrated that the pattern was a predictor of fat-poor AML in small renal masses. Recently, a study reported an "overflowing beer" sign to emphasize the diagnostic value of the portion bulging-out in fat-poor AMLs [15]. These radiologic patterns for AML could be related with tumor characteristics in terms of tissue hardness. The components of AML, such as blood vessels, smooth muscle, and adipose tissue, may contribute to a softer composition compared to RCC, in which the compact growth of malignant cells may increase the tissue hardness [24]. Tan et al. [25] distinguished AMLs from RCCs in terms of tissue characteristics by using real-time elastography. The authors demonstrated that AMLs revealed predominantly or completely soft elasticity patterns, which were substantially different from those of RCCs.

Although the reported radiologic patterns may be useful

 https://doi.org/10.3348/kjr.2020.0865

for differential diagnosis of small renal tumors, there are some limitations as follows. First, qualitative assessment based on the radiologist's decision might affect diagnostic accuracy, especially if the sign was equivocal on imaging. Kim et al. [21] utilized the ratio of long-to-short axis diameter as a semi-quantitative parameter in their diagnostic model for small renal tumors. The long-to-short axis diameter might be different between fat-poor AMLs and RCCs because the elongated feature is more common in AML. However, the parameter was not significantly different between fat-poor AMLs and RCCs in another study [22]. Furthermore, long-to-short axis diameter measured on a plane may be limited to represent entire tumor shape, because the parameter does not reflect morphologic characteristics of tumor margin. Second, the radiologic patterns revealed a relatively lower sensitivity (range, 55.1–78%) compared with specificity (range, 81.9–100%) for diagnosing fat-poor AML. In line with the previous results, the sensitivity of qualitative analysis in our study was 65.4%, which was relatively lower than the specificity (89.6%). This is because the radiologic patterns can be indistinct or even absent in some fat-poor AMLs. In our results, 9 of the 26 AMLs did not show any signs for AML. Of them, six lesions were distinguished from RCC because they revealed lower circularity index than the cut-off value. This finding may have resulted in increased sensitivity of circularity for determining AML. Therefore, we assumed that circularity could have the ability to discriminate non-round AML without distinct radiologic pattern from RCC, because circularity comprehensively reflects any morphologic characteristic that affects roundness of a tumor.

As well-known characteristics of AML, female sex and smaller tumor volume were other independent predictors of AML in our study. Although we identified the diagnostic value of circularity, the parameter might be overlapped between round fat-poor AML and non-round RCC. In our study, 9.3% and 12.8% of tumors could have been misdiagnosed according to circularity and radiologic pattern, respectively. Therefore, small round fat-poor AML remains to be a diagnostic challenge in terms of morphologic analysis. These findings may warrant a comprehensive diagnostic model utilizing clinical and variable imaging features.

There were several limitations in our study. First, fat-poor AML was defined based on the imaging finding instead of pathologic fat quantification. This is because the absence of identifiable fat in a renal tumor on unenhanced CT is clinically meaningful for malignant potential. In such cases, further radiologic modality or even intervention should be considered for differential diagnosis. Second, our results should be further validated with homogeneous CT data in a larger population. High proportion of referred films from the other hospitals resulted heterogeneous CT imaging protocols. Therefore, we could not consider non-morphologic imaging features, such as tumor texture or enhancement pattern, in our analysis. However, we think our results are still meaningful because the morphologic analysis of tumor shape may be relatively independent of imaging protocol or modality. Circularity can be easily and reliably measured if the imaging modality adequately provides a serial cross-sectional feature of a tumor. Third, we simply aimed to demonstrate the difference of circularity between fat-poor AML and RCC in this study. Although our results enlightened the utility of a quantitative shape factor, further studies to construct a diagnostic model in differentiating fat-poor AML and RCC to avoid unnecessary treatment are warranted. Fourth, we only included the three most common histological types of RCC and other miscellaneous types of renal tumors were not analyzed. This is because the majority of the pathologic decisions had been based on a previous version of the World Health Organization classification and an insufficient number of rare subtypes might result in bias. Finally, we only evaluated tumor circularity in axial images due to lack of reconstructed images especially in the referred images from other hospitals. Tumor circularity might be different in the sagittal or coronal plane in some cases; accordingly, the optimal cut-off and diagnostic power of circularity might be different. The sphericity, which is a scale of how an object closely resembles a perfect sphere in a three-dimensional space, can be considered a complementary shape factor in future studies to make up for the limitation of circularity that only represents the shape on a plane. In conclusion, circularity is a useful quantitative shape factor of small renal tumor for differentiating fat-poor AML from RCC.

Conflicts of Interest

The authors have no potential conflicts of interest to disclose.

Author Contributions

Conceptualization: all authors. Data curation: all authors. Formal analysis: all authors. Investigation: all authors. Methodology: all authors. Project administration: all

https://doi.org/10.3348/kjr.2020.0865

Korean Journal of Radiology
KJR

authors. Resources: all authors. Software: all authors. Supervision: all authors. Validation: all authors. Visualization: all authors. Writing—original draft: all authors. Writing—review & editing: all authors.

ORCID iDs
Hye Seon Kang
https://orcid.org/0000-0002-7789-8387
Jung Jae Park
https://orcid.org/0000-0002-5212-9434

REFERENCES

1. Fujii Y, Ajima J, Oka K, Tosaka A, Takehara Y. Benign renal tumors detected among healthy adults by abdominal ultrasonography. *Eur Urol* 1995;27:124-127
2. Kutikov A, Fossett LK, Ramchandani P, Tomaszewski JE, Siegelman ES, Banner MP, et al. Incidence of benign pathologic findings at partial nephrectomy for solitary renal mass presumed to be renal cell carcinoma on preoperative imaging. *Urology* 2006;68:737-740
3. Bosniak MA, Megibow AJ, Hulnick DH, Horii S, Raghavendra BN. CT diagnosis of renal angiomyolipoma: the importance of detecting small amounts of fat. *AJR Am J Roentgenol* 1988;151:497-501
4. Takahashi K, Honda M, Okubo RS, Hyodo H, Takakusaki H, Yokoyama H, et al. CT pixel mapping in the diagnosis of small angiomyolipomas of the kidneys. *J Comput Assist Tomogr* 1993;17:98-101
5. Jinzaki M, Tanimoto A, Narimatsu Y, Ohkuma K, Kurata T, Shinmoto H, et al. Angiomyolipoma: imaging findings in lesions with minimal fat. *Radiology* 1997;205:497-502
6. Kim JK, Park SY, Shon JH, Cho KS. Angiomyolipoma with minimal fat: differentiation from renal cell carcinoma at biphasic helical CT. *Radiology* 2004;230:677-684
7. Silverman SG, Israel GM, Herts BR, Richie JP. Management of the incidental renal mass. *Radiology* 2008;249:16-31
8. Fittschen A, Wendlik I, Oeztuerk S, Kratzer W, Akinli AS, Haenle MM, et al. Prevalence of sporadic renal angiomyolipoma: a retrospective analysis of 61,389 in- and out-patients. *Abdom Imaging* 2014;39:1009-1013
9. Prasad SR, Humphrey PA, Catena JR, Narra VR, Srigley JR, Cortez AD, et al. Common and uncommon histologic subtypes of renal cell carcinoma: imaging spectrum with pathologic correlation. *Radiographics* 2006;26:1795-1806; discussion 1806-1810
10. Jinzaki M, Tanimoto A, Mukai M, Ikeda E, Kobayashi S, Yuasa Y, et al. Double-phase helical CT of small renal parenchymal neoplasms: correlation with pathologic findings and tumor angiogenesis. *J Comput Assist Tomogr* 2000;24:835-842
11. Alshumrani G, O'Malley M, Ghai S, Metser U, Kachura J, Finelli A, et al. Small (< or = 4 cm) cortical renal tumors: characterization with multidetector CT. *Abdom Imaging* 2010;35:488-493
12. Sung CK, Kim SH, Woo S, Moon MH, Kim SY, Kim SH, et al. Angiomyolipoma with minimal fat: differentiation of morphological and enhancement features from renal cell carcinoma at CT imaging. *Acta Radiol* 2016;57:1114-1122
13. Verma SK, Mitchell DG, Yang R, Roth CG, O'Kane P, Verma M, et al. Exophytic renal masses: angular interface with renal parenchyma for distinguishing benign from malignant lesions at MR imaging. *Radiology* 2010;255:501-507
14. Kim KH, Yun BH, Jung SI, Hwang IS, Hwang EC, Kang TW, et al. Usefulness of the ice-cream cone pattern in computed tomography for prediction of angiomyolipoma in patients with a small renal mass. *Korean J Urol* 2013;54:504-509
15. Kim YH, Han K, Oh YT, Jung DC, Cho NH, Park SY. Morphologic analysis with computed tomography may help differentiate fat-poor angiomyolipoma from renal cell carcinoma: a retrospective study with 602 patients. *Abdom Radiol (NY)* 2018;43:647-654
16. Takashimizu Y, Iiyoshi M. New parameter of roundness R: circularity corrected by aspect ratio. *Prog in Earth and Planet* 2016;3:2
17. Choi HJ, Choi HK. Grading of renal cell carcinoma by 3D morphological analysis of cell nuclei. *Comput Biol Med* 2007;37:1334-1341
18. Schöchlin M, Weissinger SE, Brandes AR, Herrmann M, Möller P, Lennerz JK. A nuclear circularity-based classifier for diagnostic distinction of desmoplastic from spindle cell melanoma in digitized histological images. *J Pathol Inform* 2014;5:40
19. Murphy GF, Partin AW, Maygarden SJ, Mohler JL. Nuclear shape analysis for assessment of prognosis in renal cell carcinoma. *J Urol* 1990;143:1103-1107
20. Nanes BA. Slide set: reproducible image analysis and batch processing with ImageJ. *Biotechniques* 2015;59:269-278
21. Kim MH, Lee J, Cho G, Cho KS, Kim J, Kim JK. MDCT-based scoring system for differentiating angiomyolipoma with minimal fat from renal cell carcinoma. *Acta Radiol* 2013;54:1201-1209
22. Takahashi N, Leng S, Kitajima K, Gomez-Cardona D, Thapa P, Carter RE, et al. Small (< 4 cm) Small (< 4 cm) renal masses: differentiation of angiomyolipoma without visible fat from renal cell carcinoma using unenhanced and contrast-enhanced CT. *AJR Am J Roentgenol* 2015;205:1194-1202
23. Park JJ, Kim CK. Small (< 4 cm) renal tumors with predominantly low signal intensity on T2-weighted images: differentiation of minimal-fat angiomyolipoma from renal cell carcinoma. *AJR Am J Roentgenol* 2017;208:124-130
24. Dyer R, DiSantis DJ, McClennan BL. Simplified imaging approach for evaluation of the solid renal mass in adults. *Radiology* 2008;247:331-343
25. Tan S, Özcan MF, Tezcan F, Balci S, Karaoğlanoğlu M, Huddam B, et al. Real-time elastography for distinguishing angiomyolipoma from renal cell carcinoma: preliminary observations. *AJR Am J Roentgenol* 2013;200:W369-W375

 https://doi.org/10.3348/kjr.2020.0865